Jarno Saruaho

Cables' Modeling Methodology for Mechanical Simulations

Metropolia University of Applied Sciences

Bachelor of Engineering

Mechanical Engineering

Bachelor's Thesis

24 May 2022

Abstract

Author:	Jarno Saruaho
Title:	Cables' Modeling Methodology for Mechanical Simulations
Number of Pages:	28 pages
Date:	24 May 2022
Degree:	Bachelor of Engineering
Degree Programme:	Mechanical Engineering
Professional Major:	Machine Design
Supervisors:	Jyrki Kullaa, Principal Lecturer Pertti Poskiparta, Lead CAE Engineer (Mechanical Simulation)

In this thesis, a methodology for modeling high voltage and cooling cables, which are included in mechanical simulations for complete battery pack assemblies, was developed. The simulations in this thesis were performed with Altair OptiStruct and RADIOSS software. Only the static cases were considered.

The aim of this thesis was to develop a reliable and efficient methodology, which consists of physical testing of cables, development of the cable modeling method in a simulation environment, creation of a material model for the cable and verification of the physical test results.

Physical testing of the cables included uniaxial tensile, three-point bend and crush tests. Three-point bend and crush tests were reproduced in a simulation environment to verify the physical test data using the new modeling method for the cables.

The satisfying results were acquired from all the other physical tests except tensile tests. There were some problems in gripping the cables with self-tightening jaws. Despite that, the new modeling method turned out to be quite fast and easy to use. Reproducing the physical test results in simulation environment with the new modeling method went partially as wanted. There was deviation, but the FEA curve followed the physical test curves' shapes nicely. This means that some refining is still needed for the methodology to make it meet the desired needs.

Keywords: FEA, FEM, Material testing, Mechanical simulation

Tiivistelmä

Tekijä:	Jarno Saruaho
Otsikko:	Cables' Modeling Methodology for Mechanical Simulations
Sivumäärä:	28 sivua
Aika:	24.5.2022
Tutkinto:	Insinööri (AMK)
Tutkinto-ohjelma:	Konetekniikka
Ammatillinen pääaine:	Koneensuunnittelu
Ohjaajat:	Yliopettaja, Jyrki Kullaa Lead CAE Engineer (mekaaninen simulointi), Pertti Poskiparta

Työssä kehitettiin metodologia suurjännite- ja jäähdytyskaapeleiden mallintamiseen, jotka sisältyvät mekaanisiin simulaatioihin ja jotka tehdään kokonaisille akkukokoonpanoille. Työhön liittyvät simuloinnit suoritettiin Altair OptiStruct- sekä RADIOSS-ohjelmistoilla. Vain staattisia tapauksia käytiin läpi.

Työn tavoitteena oli kehittää luotettava ja tehokas metodologia, joka koostuu kaapeleiden fyysisestä testauksesta, kaapeleiden mallinnustavan kehittämisestä simulaatioympäristössä, materiaalimallien luonnista kaapeleille sekä fyysisten testitulosten verifioinnista.

Kaapeleiden fyysiseen testaukseen sisältyi veto-, taivutus- sekä puristustestit. Kolmepistetaivutus- sekä rutistustesti jäljennettiin simulaatioympäristössä, jotta niiden fyysinen testidata saatiin verifioitua kaapelien uudella mallinnustavalla.

Tässä opinnäytetyössä saatiin tyydyttävät tulokset kaikista muista fyysisistä testeistä paitsi vetokokeista. Kaapeleihin tarttumisessa itsekiristyvien leukojen kanssa oli ongelmia. Siitä huolimatta uusi mallinnusmenetelmä osoittautui melko nopeaksi ja helppokäyttöiseksi. Fyysisten testien tulosten toistaminen simulaatioympäristössä uudella mallinnusmenetelmällä sujui jokseenkin toivotulla tavalla. Poikkeamaa oli, mutta FEA-käyrät seurasivat hienosti fyysisten testikäyrien muotoja. Tämä tarkoittaa sitä, että metodologia tarvitsee vielä jonkin verran hiomista, jotta se vastaa haluttuja tarpeita.

Avainsanat: FEA, FEM, Materiaalitestaus, Mekaaninen simulointi

Contents

List of Abbreviations

UTS: Ultimate tensile stress. Maximum engineering stress before necking starts to happen (ductile materials) or failure happens (brittle materials).

YS: Yield Stress. Stress point what indicates when materials elastic area ends, and plastic area starts.

FEA: Finite Element Analysis. Simulation of different physical applications using numerical technique called Finite Element Method (FEM).

TCL: Tool Command Language. Programming language.

UTM: Universal Testing Machine. Testing machine that is used to determine mechanical properties of a test specimen through physical tests (e.g., tensile and compression tests).

DOF: Degrees of Freedom. Number of variables in mechanical system, that define its state.

1 Introduction

When thinking about what you need for finite element analysis (FEA), the two main things that come up, are proper material data for material cards and efficient modeling (meshing) method with the use of suitable finite elements. Material data can be acquired through multiple physical tests with the help of universal testing machine (UTM). The selection and usage of the right finite elements comes usually through experience and testing of the model.

This thesis was performed as a development project for Valmet Automotive EV Power Oy. The goal was to build a reliable and efficient methodology for modeling high voltage and cooling cables, which are included in mechanical simulations done for complete battery pack assemblies with Altair OptiStruct or RADIOSS. Some cases that the finished cable model will be involved are shock and vibration simulations. The desired methodology involves physical testing of the cable, translating the test data to required format to generate proper material model, setting up tests in simulation environment for verifying the data and modeling of the cables. Only one type of a single core high voltage cable used in automotive battery pack, was handled in this thesis. Idea was that the finished product of the methodology could then be implemented on other cable types.

Main reasons for this project were that the material data of the cables were too scarce to produce precise results from simulations, and the modeling method required too many unnecessary finite elements. This was the problem especially with longer cables. With some of the cables being so heavy, development of the methodology was truly needed in the aspect of getting proper behavior of the cables. It was agreed that only the static testing was performed for this thesis, and that the dynamic testing could be done later.

2 Theory of physical testing for FEA

Acquiring accurate results from FEA requires using proper material data, and when testing mechanical behavior of materials for FEA, the most common test is uniaxial tensile test (longitudinal pull test). That test alone produces ~90 % of the needed data for FEA. [5, p. 7] Some important data that can be acquired are ultimate tensile stress (UTS), yield stress (YS), Young's modulus and force-elongation data. Knowing the point of UTS is important, with it being the highest value of engineering stress (*U* in Figure 1). In addition to that, when reaching UTS, with most ductile materials, the necking begins and with brittle materials failure happens. [1, p. 36,40] In the theory of this thesis the focus stays with linear elastic ductile materials.

In the product design process, YS plays an important role. That is because before passing it, the deformation is elastic (material returns to original shape), and after that it is plastic until reaching UTS (the deformation is permanent). This provides an option to perform the whole design phase in the elastic region, in order to avoid the design from passing the yield point. Sometimes it might be difficult to determine the point of YS, and for that reason a common way to do it, is to draw an offset line from the linear portion of the stress-strain curve. As seen in Figure 1, the dashed line starts from 0,002 (0,2 %) strain, and the intersection of this line and the stress-strain curve is the offset YS point (*Y* in Figure 1). [1, p. 37-39]

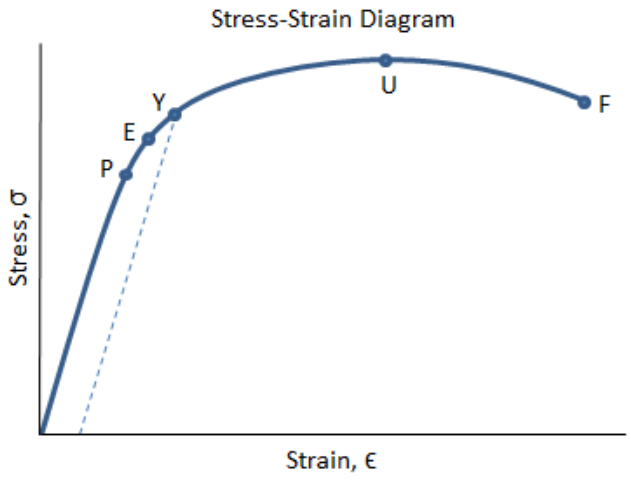

Figure 1 Stress-strain curve for some ductile material with labels. [3]

When there is a linear part before YS in the beginning of stress-strain curve (from origin to *P*, in Figure 1), Young's modulus (or elastic modulus) E can be calculated from that with Equation 1. This equation is from Hooke's Law. [2, p. 22-23]

$$\sigma = E\varepsilon \leftrightarrow E = \frac{\sigma}{\varepsilon} \quad (1)$$

The materials with difficulty to determine Young's modulus, have become more common (e.g., plastics and rubbers), and as you can see from Figure 2, there are numerous ways to determine the Young's modulus.

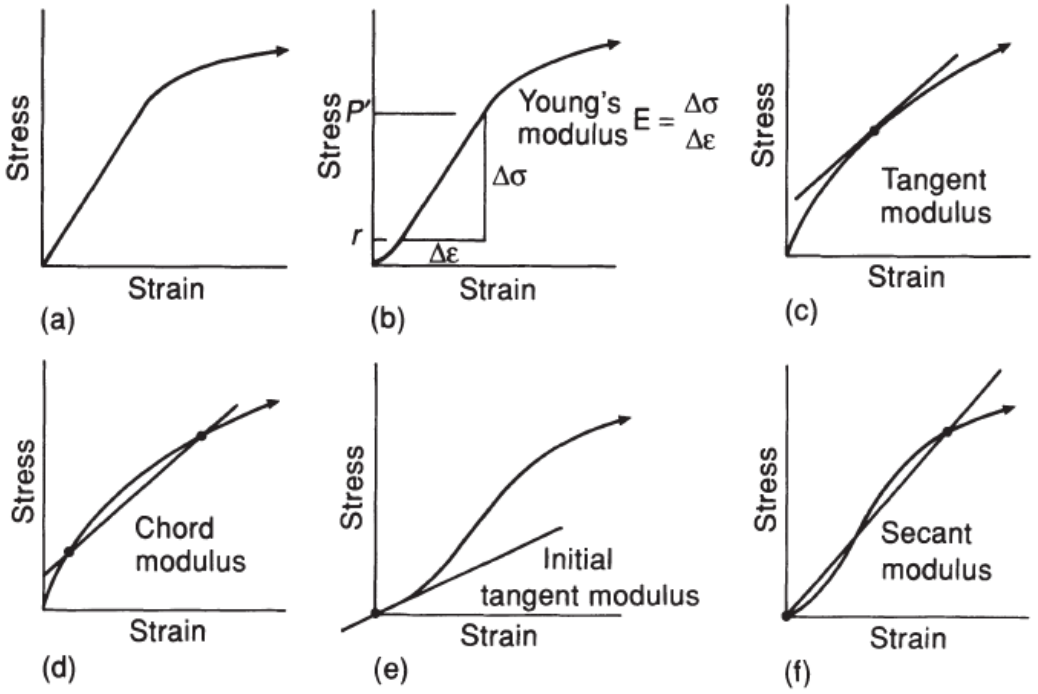

Figure 2 Different ways to determine Young's modulus. [6, p. 151]

There is also flexural modulus (or bending modulus) that can be acquired through three- or four-point bending test [9,10], and in addition to that, there is also compression modulus, that can be obtained with compression test [11]. When the test sample's geometry is complicated, e.g., in the case of this thesis, it seems more practical to perform physical tests, rather than calculate these moduli by hand. In both tests, stress-strain curve is formed, and modulus is calculated almost in same manner as Young's modulus shown above.

Force-elongation data from testing is converted by converting the forces F to stresses σ (Equation 2) and elongations L/L_0 to strains ε (Equation 3).

$$\sigma = \frac{F}{A_0} \tag{2}$$

$$\varepsilon = \frac{\Delta L}{L_0} = \frac{L - L_0}{L_0} \tag{3}$$

After that the stress-strain data is used to build an engineering stress-strain curve, and furthermore that can be transformed into a true stress-true strain curve (Figure 3). In engineering curve, you assume that the original cross-section A_0 stays the same for the whole test, and for the true curve it is the opposite. The translation from engineering to true curve is done with Equations 4 and 5. These equations are valid only if the deformation is equally distributed along the gauge section. Despite the accuracy of true curve, after necking starts, cross-section must be measured during the test to get the right results. [1, p. 41-42]

$$\sigma_{true} = \sigma(1 + \varepsilon) \tag{4}$$

$$\varepsilon_{true} = \ln(1 + \varepsilon) \tag{5}$$

As Petrík and Ároch [4] has shown, the use of undeformed cross-section in engineering curve provides inaccurate results, and therefore the use of true curve is always recommended.

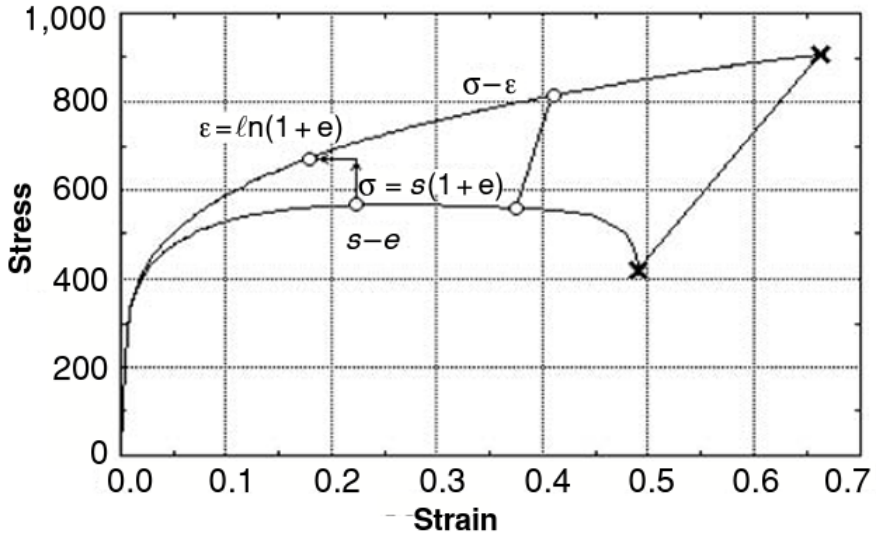

Figure 3 Difference of engineering (s-e) and true (σ-ε) stress-strain curves. [1, p. 42]

Poisson's ratio ν (Equation 6) is crucial for simulations because it gives you the ratio between axial strain and lateral contraction. The measurement is simple with isotropic materials when ratio is the same for all directions, but e.g., with anisotropic materials it becomes a bit more difficult with the ratio being non-uniform in all directions. [5, p. 27-28]

$$\nu = -\frac{\Delta\varepsilon_{lateral}}{\Delta\varepsilon_{axial}} \quad (6)$$

Properties said before are already more than enough to create simple material models. For example, when creating an isotropic linear elastic material model for linear static analysis, the only material properties needed are [12]:

- Density
- Poisson's ratio
- Young's modulus

And even the use of density isn't needed if the analysis doesn't use mass elements. So, the only two mandatory material properties for simulations (excluding thermal simulations), are Poisson's ratio and Young's modulus. [12] But as a comparison, a common way to create ideal isotropic elastoplastic material model for nonlinear analyses in RADIOSS, is to use the following parameters [15]:

- Ultimate tensile stress (UTS)
- Engineering strain at UTS
- Yield stress (YS)
- Density
- Poisson's ratio
- Young's modulus

If one does not have access to comprehensive material databases, usually the only values to be found are the ones shown above. There are many different material cards as well as parameters to choose from, but with its topic so broad, it's not appropriate to go through them within this thesis.

3 Introduction to FEM

This chapter will go through briefly the basics of FEM. For example, what are finite elements and how they are formed as well as what kind of different approaches there are when solving a problem with FEM, are introduced. Below in Figure 4 is probably the most known part about FEM, mesh formed with elements and results shown in the form of heat map. Usually, FEA is used to solve displacements and stresses of structures, but there is also a possibility to solve e.g., heat-transfer as well as fluid mechanics problems using FEM. [18, p. 7]

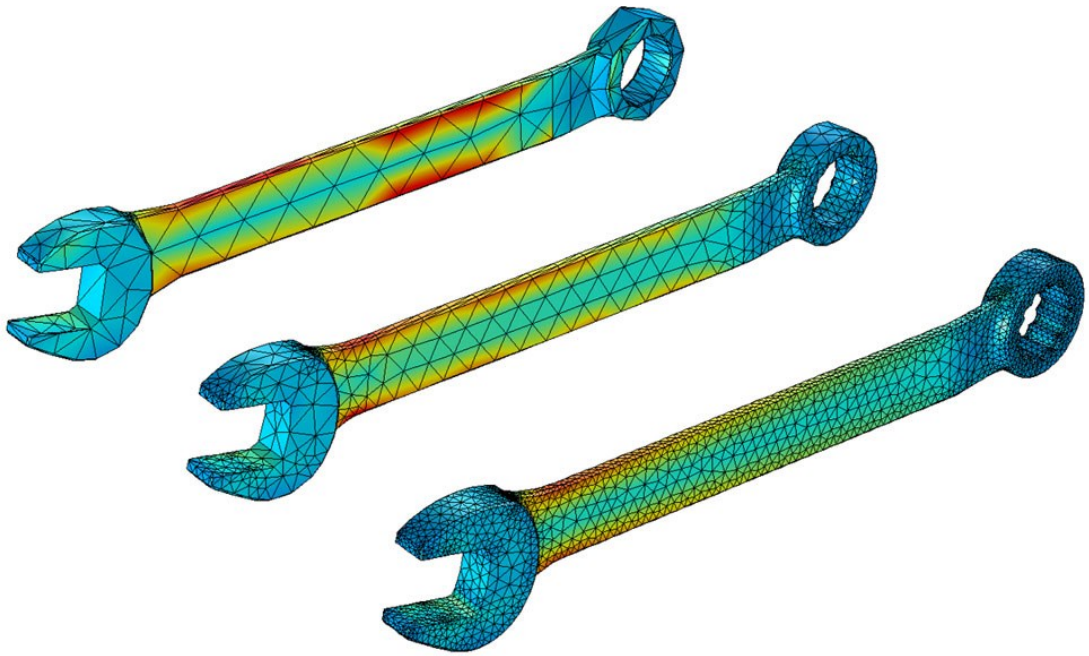

Figure 4 Iterations of a wrench modeled (meshed) with finite elements. [19]

When approaching structural mechanical problems with FEM, there are two typical direct approaches, the stiffness (displacement) method where you assume the displacement of the nodes to be the unknowns of the problem, and the flexibility (force) method where you assume the forces to be the unknowns. It has been made studies that shows the displacement method being more desirable computationally than the force method. The reason for this is the formulation being simpler for most structural problems with the displacement method. There are also variational methods that can be used, the theorem of minimum potential energy and the principle of virtual work. [18, p. 7-8]

Problem solving starts with discretizing (modeling/meshing) the structure with appropriate elements and choosing the right size for them in different areas of the part/structure. When choosing the size of the elements, you must keep in mind that the elements must be small enough to get desired results and large enough to give efficient calculation time. Modeling is usually based on a 3D-model geometry, but simple 1D and 2D structures can be modeled with the help of temporary geometry done in the pre-processor (in Altair software). Figure 5 shows general elements used in FEM. As you can see there are dots in every corner of the elements, those are called nodes, and with those, elements are connected to each other. [18, p. 8-9]

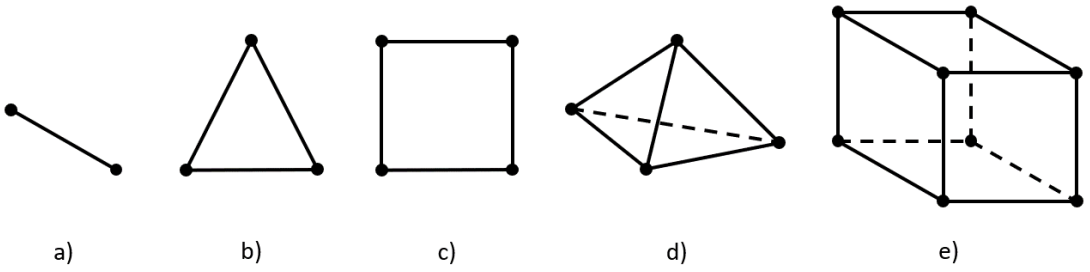

Figure 5 Illustration of different general elements used in FEM: a) two-noded 1D line element, b) three-noded 2D tria element, c) four-noded 2D quad element, d) four-noded 3D tetra element, e) eight-noded 3D hexa (or brick) element.

Next step is to decide a displacement function within each element. That is defined by using the nodal values of the element. As an example, in 2D-problem for 2D-element in the x-y plane, the functions are formed with the nodal unknowns (x and y components). Strain/displacement and stress/strain relationships are also needed for deriving the equations for the elements. E.g., if there is deformation in the x direction, there is strain ε_x happening because of displacement u. This can be calculated with Equation 7 (for small strains). [18, p. 11]

$$\varepsilon_x = \frac{du}{dx} \tag{7}$$

This leads to stresses that are related to the strains. The simplest way to acquire stress is to utilize Hooke's law (Equation 8), that was introduced earlier in Chapter 2. [18, p. 11]

$$\sigma_x = E\varepsilon_x \tag{8}$$

Now that all the other functions are formed, the next step is to build the element stiffness matrix and equations with the approaches mentioned earlier. For 1D elements (*a* in Figure 5) the easiest methods to apply are the direct equilibrium methods (displacement method as well as force method). When dealing with 2D and 3D elements (*b*-*e* in Figure 5), more suitable methods are the work and energy methods (e.g., principle of minimum potential energy and principle of virtual work). Nevertheless, whichever method you are using, it will produce the needed equations to describe the behavior of the element. The equations are then written in matrix form as shown in Equation 9. [18, p. 11-13]

$$\{f\} = [k]\{d\} \rightarrow \begin{Bmatrix} f_1 \\ f_2 \\ \vdots \\ f_n \end{Bmatrix} = \begin{bmatrix} k_{11} & k_{12} & \cdots & k_{1n} \\ k_{21} & k_{22} & \cdots & k_{2n} \\ \vdots & \vdots & \ddots & \vdots \\ k_{n1} & k_{n2} & \cdots & k_{nn} \end{bmatrix} \begin{Bmatrix} d_1 \\ d_2 \\ \vdots \\ d_n \end{Bmatrix} \tag{9}$$

$\{f\}$ is vector of nodal forces in the element $(n \times 1)$
$[k]$ is element stiffness matrix $(n \times n)$
$\{d\}$ is vector of nodal DOF in the element $(n \times 1)$
n is total number of nodal DOF in the element

When there are matrices formed for all the elements, the global equations are formed from those, e.g., global stiffness matrix (Equation 10). [18, p. 13-14]

$$\{F\} = [K]\{d\} \tag{10}$$

$\{F\}$ is vector of global nodal forces $(N \times 1)$
$[K]$ is global stiffness matrix $(N \times N)$
$\{d\}$ is vector of nodal DOF in the structure $(N \times 1)$
N is total number of nodal DOF in the structure

At this stage, it can be displayed, that the global stiffness matrix $[K]$ is singular matrix ($det[K] = 0$). This problem is solved by determining some boundary conditions (or constraints), such as the structure stays still and does not move around as rigid body. When the known constraints are placed to the global equations, you can solve the equations for the unknown DOFs by elimination method (e.g., Gauss's method) or iterative method (e.g., Gauss-Seidel method). Final step before analyzing the results is to solve for the strains and stresses in the elements. For example, this can be done with Equations 7 and 8. [18, p. 14]

4 Physical testing of cables

Physical testing of materials/products have a big role in acquiring proper behavior data of the material/product (in this thesis the cables, that you can see in Figure 6). As Baeker [13] states, the simulation results cannot be more accurate than the input data itself. Performing the testing inside the company was a big motivation to start developing the methodology and the kick-off of this thesis. The fact that testing is done internally in the company, produces the results much cheaper, and gives more freedom on what to do. Plans of tests and test setups were already done before this thesis, but they needed some final refinements to make them complete.

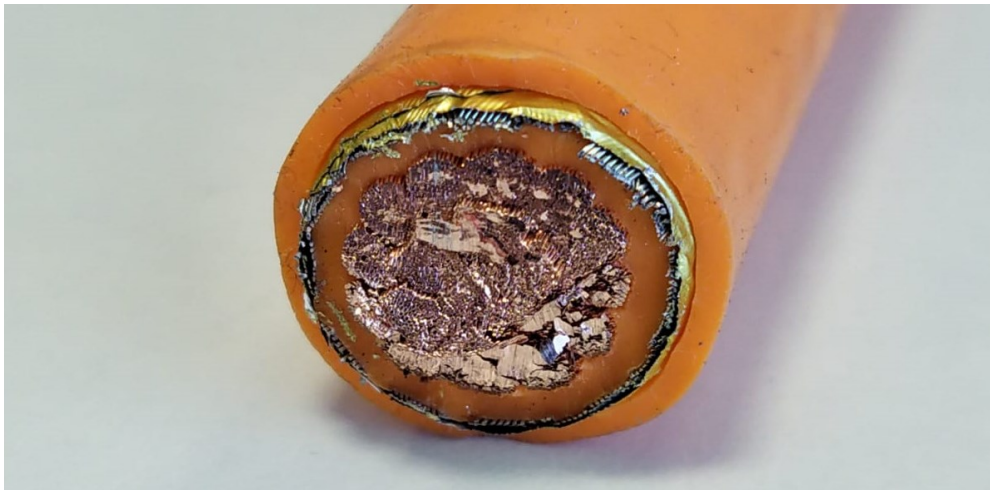

Figure 6 Cross-section of the test specimen.

The tests done in this thesis were performed at Valmet Automotive's laboratory located in Uusikaupunki. The testing jigs used in the tests were modeled and manufactured just for these tests (also inside the company). Doing this meant that in the same process, 3D-models from the jigs were created. Those 3D-models were used later when verifying the results in simulation environment (more in Chapter 6). The other good reason for the decision to manufacture the jigs internally, was the shipping duration of the jigs from the importer (about ten weeks). You can see more information of the test specimen, test equipment and the tests done from Table 1 and Figure 6. The values of the plots shown in this thesis are left out on purpose (at the request of the company). The results from the tests are covered more thoroughly in Chapter 6.2.

Table 1 Information of the test specimen tested.

Test specimen	Shielded single core high voltage cable		
Diameter d_0 (mm)	20,9		
Weight (g/m)	1150		
UTM	ZwickRoell Z020 TN ProLine		
Load cell of UTM (kN)	20 (max)		
Tests	Uniaxial tensile test	Three-point bending	Crush
Test speed (mm/min)	25	100	10
No. of specimens	7	7	7

There was plenty of cable ready to be used, therefore it was decided that seven specimens would be tested for each test, instead of original number of five. The quantity of five for the test specimens comes from earlier internal testing in the company. The testing speeds aren't final speeds that are determined to be the best ones to produce optimal results. These are some general values with some of them being also from earlier testing done internally in the company.

4.1 Uniaxial tensile test

Uniaxial tensile test is performed to a test specimen by holding it still from one end and pulling it from the other [16]. In Chapter 2, it was explained which kind of results you can acquire from performing a uniaxial tensile test. There were some doubts about gripping the cables with self-tightening jaws (no other gripping methods were available internally in the company). Since there does not exist a lot of force all the way from the beginning, the top insulating layer (can be seen in Figure 6) might slip, and therefore not produce correct results.

Tensile tests were performed with the help of SFS-EN ISO 6892-1:2019:en - standard [16] and the operating manual for the UTM [17]. Illustration of the tensile test setup can be seen below in Figure 7.

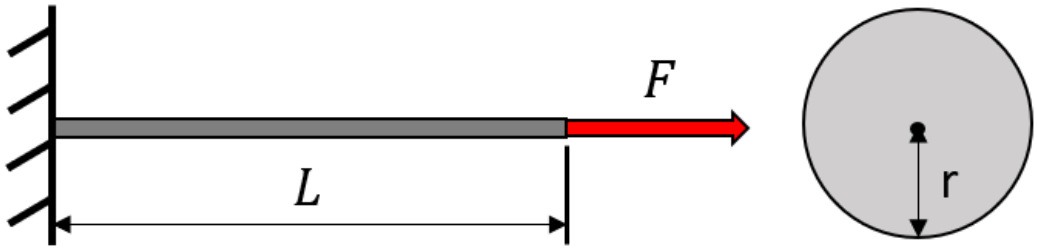

Figure 7 Illustration of test setup for tensile testing.

When determining length of the test specimens, gauge length and gripping length were needed. Gauge length L_G was calculated with Equation 11, where $k = 5{,}65$ is internationally adopted value for coefficient of proportionality, and A_0 is the original cross-sectional area [16]. As for gripping length $L_{grip,min}$, in the operating manual for the UTM used, it's recommended, that it's at least $\frac{2}{3}$ of the length of the jaw [17].

$$L_G = k\sqrt{A_0} = 5{,}65\sqrt{A_0} \tag{11}$$

In addition to that, the minimum length of the test piece between the gripping jaws L_C was calculated as follows [16]:

$$L_C = L_G + \frac{d_0}{2} = 5{,}65\sqrt{\pi\left(\frac{20{,}9}{2}\right)^2} + \frac{20{,}9}{2} \approx 70\ mm \tag{12}$$

The calculation of the minimum total length of the test specimen was done with Equation 13, where two times the minimum gripping length $L_{grip,min}$ was added to the result of Equation 12.

$$L_{cable,min} = L_C + 2L_{grip,min} = L_C + 2\left(\frac{2}{3} * 50\ mm\right) \approx 137\ mm \tag{13}$$

This calculated minimum length of the cable is shorter than the cables used in three-point bending (will be explained later), therefore the length of the test specimens used in tensile test could be the same as in three-point bending, making length between jaws $L_C = 70\ mm$ and gripping length $L_{grip} = 40\ mm$.

There was some uncertainty of testing the cable with the top insulating layer (as said above), therefore some preliminary tests were done. Below in Figure 8 you can see clear difference between a cable with and without the top insulating layer.

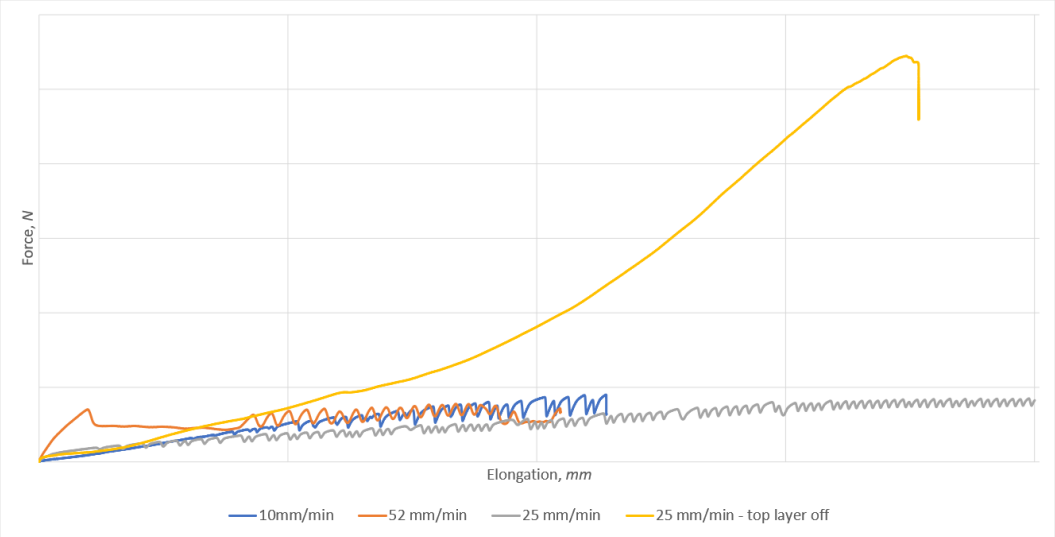

Figure 8 Force-elongation curves from calibration of testing rate for tensile testing.

A decision was made to strip the top insulating layer from all the test specimens, so that proper results could be achieved. Results from the tests fit well together, as can be seen below in Figure 9.

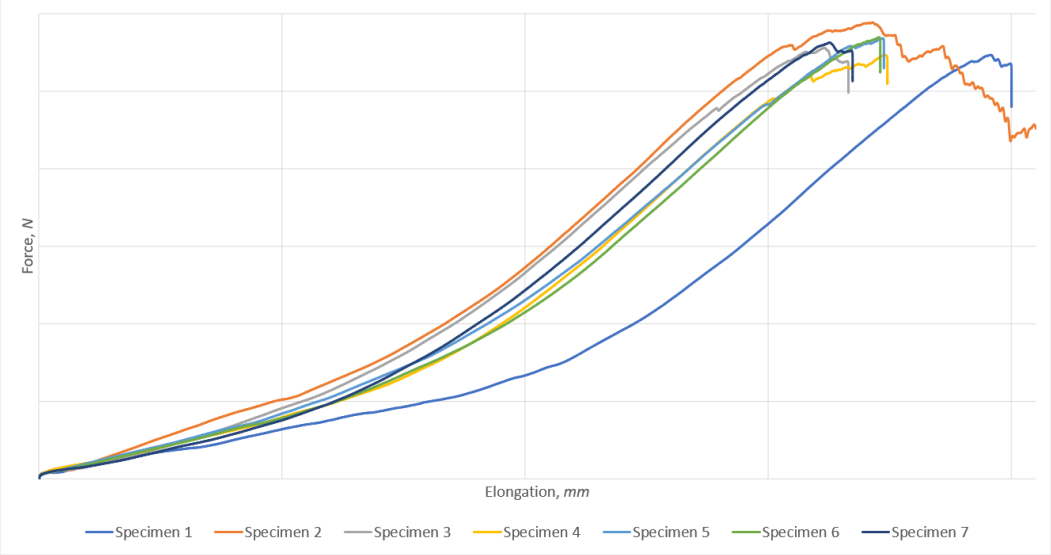

Figure 9 Force-elongation curves from the tensile tests.

From Figure 10 below, you can see the standard deviation of the results from tensile testing (excluding specimen one), with the largest deviation to the mean value being 156,05 *N*.

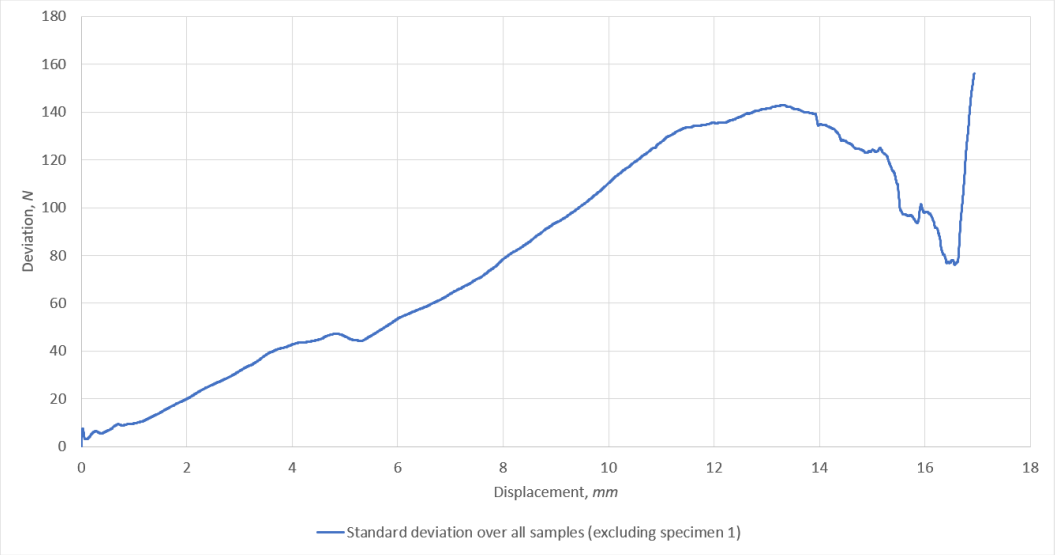

Figure 10 Standard deviation of results from tensile tests.

4.2 Three-point bend test

In three-point bending, you support a test specimen with two supports and apply force to the middle of the supports [9]. As explained in Chapter 2 you can acquire flexural modulus from the test, but you can also perform this test just to see how the test specimen behaves, and then use the results as a reference. The test setup for three-point bending performed in this thesis can be seen below in Figure 11.

Test specimen length of 150 mm and distance between supports of 100 mm, came from earlier testing made internally in the company. These values are giving a good start to develop the methodology and further testing with different values might be performed.

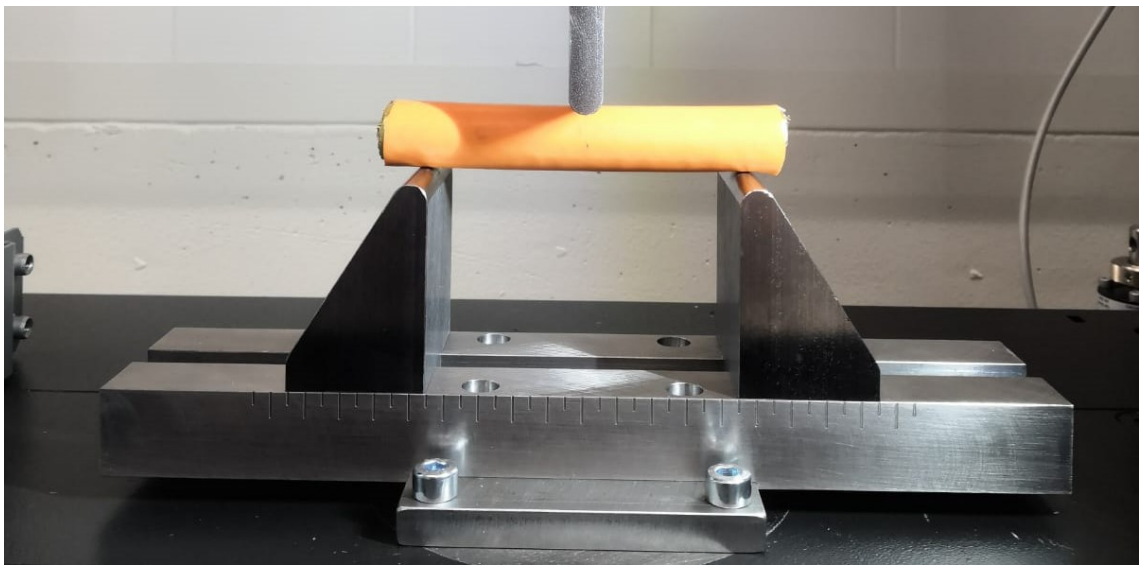

Figure 11 Three-point bending test setup used in this thesis.

Three-point bending tests went well, and no real problems occurred. As can be seen from Figure 12, there is some deviation between the results, but not anything too serious. Only two specimens produced results a bit off from the rest of five.

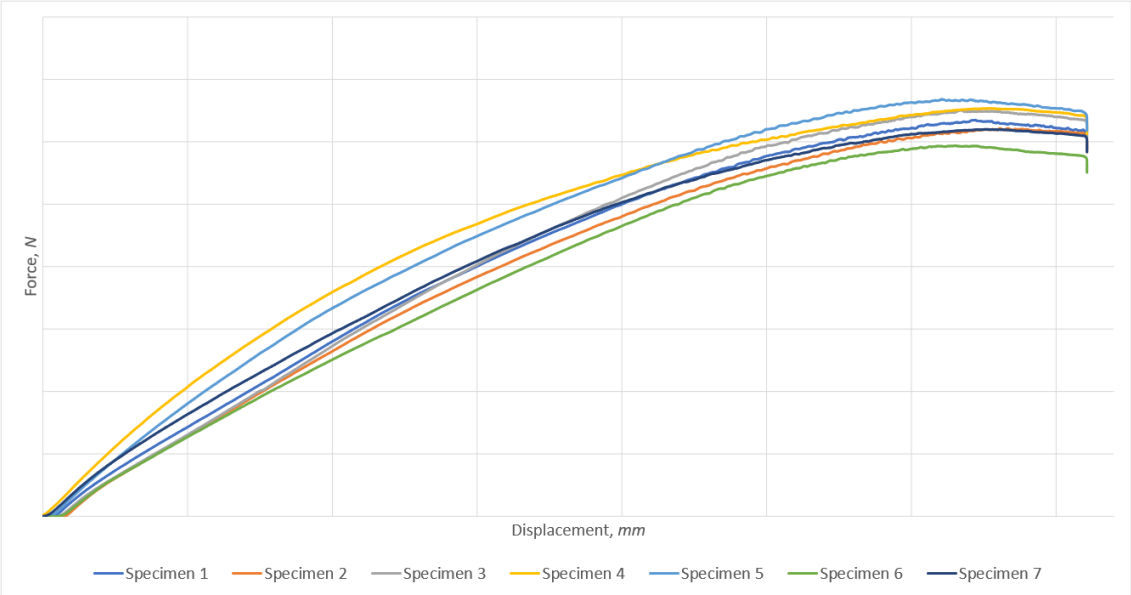

Figure 12 Force-displacement curves from three-point bend tests.

Figure 13 below confirms quite well, that without specimens four and five the deviation of the results would have been smaller, with the largest deviation to the mean value being 18,16 *N*.

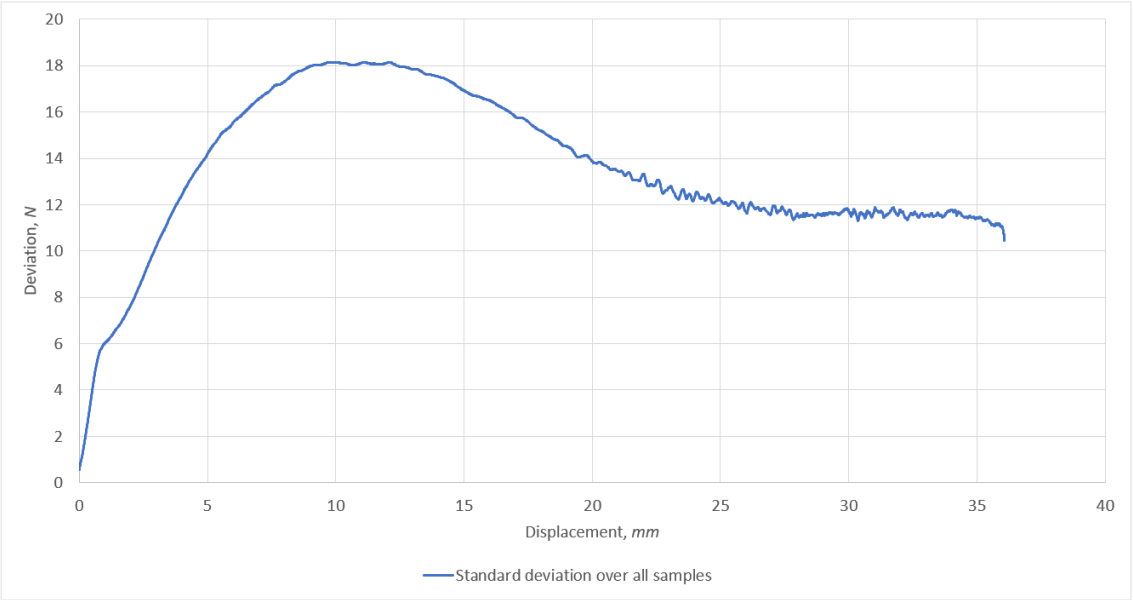

Figure 13 Standard deviation of results from three-point bend tests.

4.3 Crush test

Crush (or compressive) testing is usually done by pressing a test specimen with a plate against a level [11]. In this thesis, the crush test was done by pressing the cables in the middle against a level. The test setup for crush testing performed in this thesis can be seen below in Figure 14.

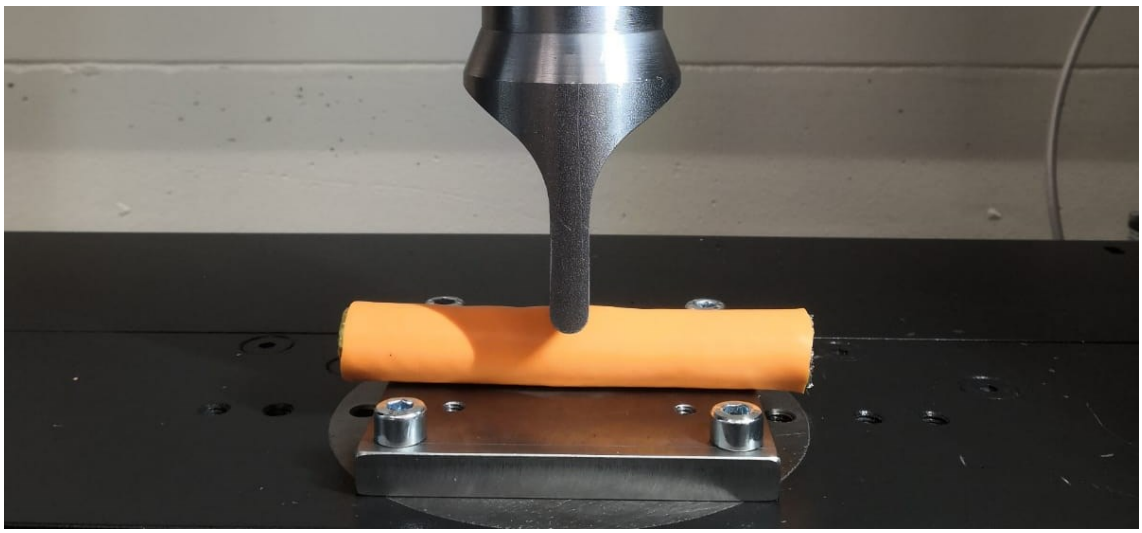

Figure 14 Crush test setup used in this thesis.

From crush tests, only the force-displacement -data was the desired output (this will be explained in detail in Chapter 5). Therefore, no transformation of data

was needed. Below in Figure 15, the results fit well together, making them all eligible.

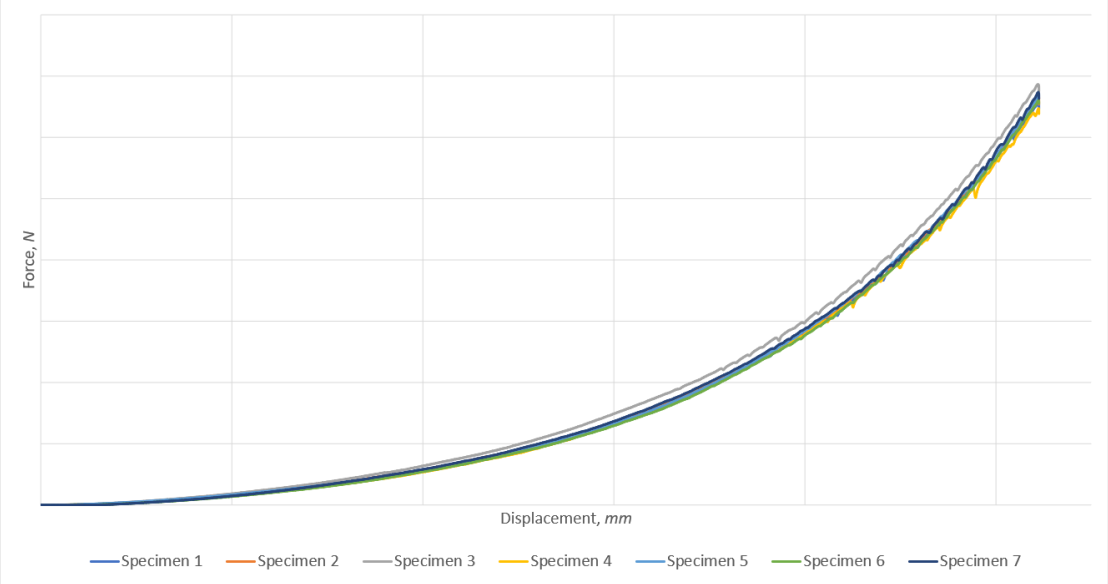

Figure 15 Force-displacement curves from the crush tests.

As for the crush tests, below in Figure 16, you can see the standard deviation being consistent until the end, with the largest deviation to the mean value being 71,37 *N*.

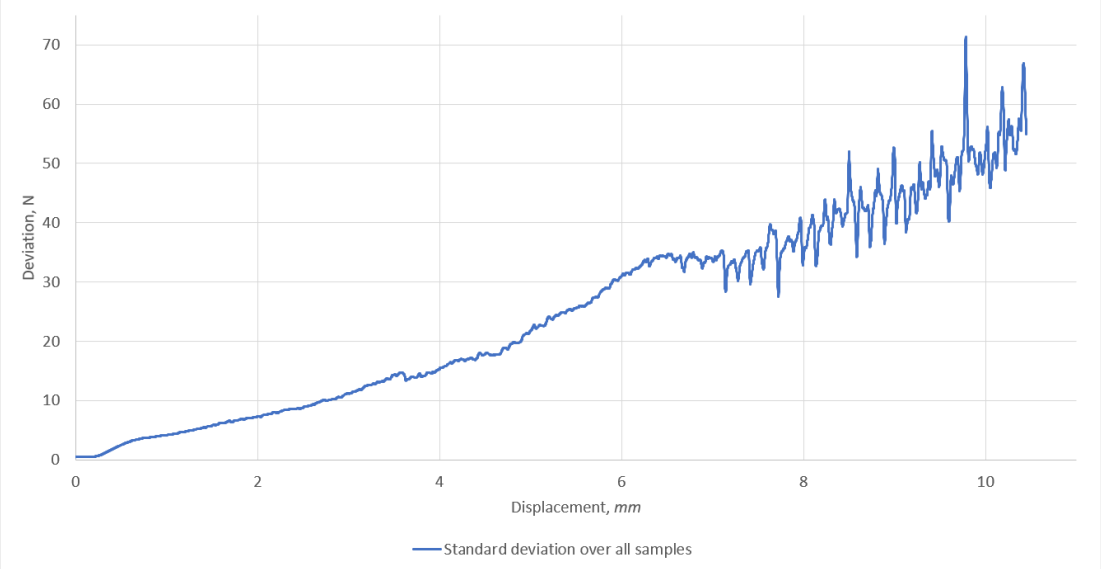

Figure 16 Standard deviation of results from crush tests.

5 Cable modeling improvement

Approach for the modeling improvement was to make the cable modeling/ meshing simpler and more efficient and to decrease the number of elements in the cable models, thus making simulation time to decrease. The old modeling method (*a* in Figure 17) was done completely with 8-noded hexahedral solids (*e* in Figure 5). The decision was that the method is too heavy computationally, compared to the impact it has on the complete battery pack assembly.

The use of 1D-elements instead of solid-elements, especially beam-elements (*a* in Figure 5) as the core of the cable, was decided immediately in the beginning. The reason for this is that in this case there is no need to acquire specific location of stresses that you get with 2D- and 3D-elements, in addition with the capability of beam-elements to model torsion, bending and axial cases of simple structures quite well [7]. The modeling of the cable can be done with beam-elements, but the problem is that they do not support modeling of deformation and contact through the cross-section. There is a way to model the thickness of a 1D-beam element through contact gaps, but that does not give the deformation in compression. This was solved by surrounding the core beams with outer shell-elements (*c* in Figure 5) that connect to them with spring-elements (*a* in Figure 5). The shells are thought as contact elements (very small thickness → small mass), and the springs will model the compression with the force-displacement data from the crush test done for the cables.

The physical test results in Chapter 4 shows well, how difficult the modeling of the part is. This is due to the fact that the part itself is not homogeneous, and it contains different materials. Figure 6 displays the cross-section of the cable, and from that you can see that there are two insulating layers made from silicone, one braided shielding layer made from some metal and the inner core made of stranded copper wires. The combination of these materials results in rather non-linear behavior, as seen in Figure 15. This is at least partially because of nonlinearly behaving silicone layers and the fact that the layers stick to each other only by friction. Nonlinear behavior was modeled with nonlinear springs and using nonlinear Young's modulus for the 1D-beam elements.

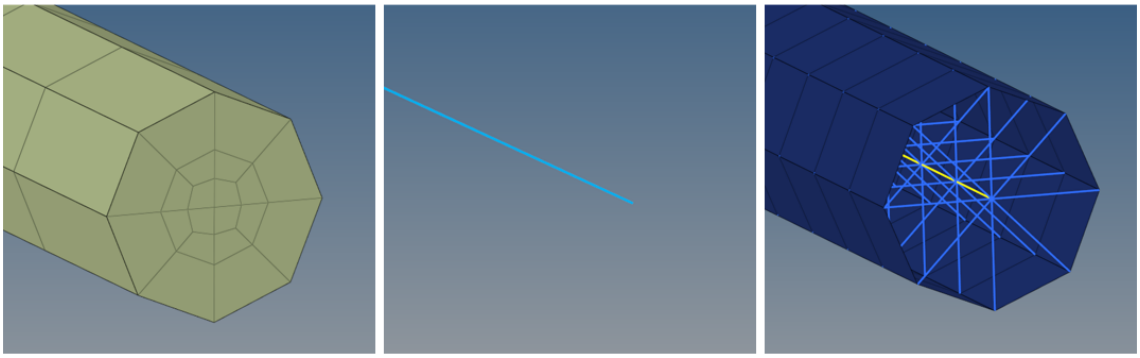

a) b) c)

Figure 17 a) Old (solids), b) beam and c) new modeling method for the cables.

When the methodology was looked from efficiency point of view, a modeling/ meshing -script was written with Tool Command Language (TCL), for both OptiStruct and RADIOSS. The script builds a complete cable with elements, element-properties, and geometry, based on a center line of the cable geometry. Material property assignment is done afterwards. Inputs that the user must give for the script are:

- Cable radius
- Center line of the cable
- End node of the center line
- Element length
- Element density on the circumference

Both static and dynamic simulations were done for three modeling methods (Figure 17), to compare how the decrease in element count with the use of 1D and 2D elements would affect the simulation time and how the new model performs in action. Basic pull and bend tests (Figure 18) were performed, and the material used in this comparison was general aluminum 2011-T3 [8]. More specific test information can be seen in Table 3. As mentioned, the new modeling method is meant to be used in both OptiStruct and RADIOSS solvers, and therefore the tests were done with both solvers. Full accuracy of the model (especially the behavior of the springs) cannot be seen without the test data from physical testing. Therefore, the accuracy of the new modeling method will be looked more precisely in Chapter 6 with the help of physical test data and more detailed simulation test setups made to represent the physical tests.

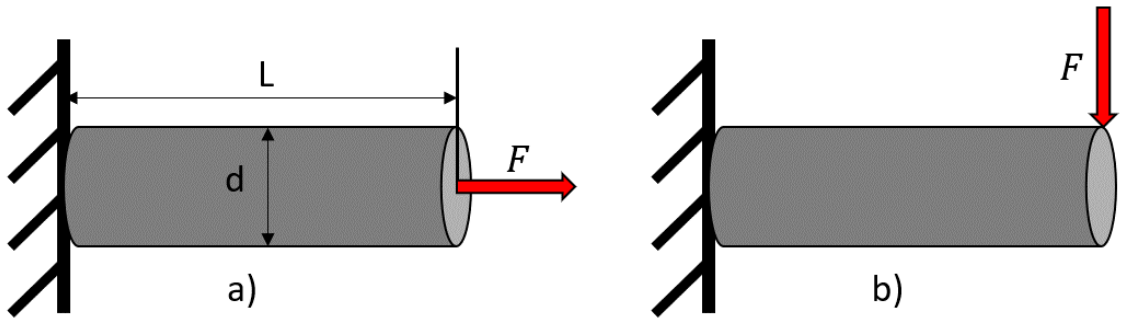

Figure 18 Illustration of a) pull and b) bend tests performed in the comparison.

In Table 2 below, you can see the number of nodes in each model used in the comparison tests. Reduction of 64 % in the node count for the new method was quite good result as well. This is not the most important thing that was changed, but rather that the number of DOFs was reduced. The reason for this is, if the number of DOFs grows, the bigger the global stiffness matrix $[K]$ is formed, and therefore making it heavier computationally. Equations 9 and 10 display well how the global matrix is formed and how the size for the matrix is determined. [14, 15]

Table 2 Element and node counts in the models for the comparison tests.

Element size (mm)	Modeling method	Element count	Node count
10	Solids (old)	200 hexas	275
	Beams	10 beams	11
	New	80 shells + 88 springs + 10 beams	99
5	Solids (old)	400 hexas	525
	Beams	20 beams	21
	New	160 shells + 168 springs + 20 beams	189

Doing a static simulation in the beginning of a new model is always a good way to check if the model is working as intended. As the basic function in static cases is $\sum F = 0$, the calculation is not as demanding as with dynamic cases. Compared to static case, the basic function in dynamic case is $\sum F = ma$, as

acceleration and mass are considered. With the new modeling method, dynamic case is more likely the case that it will be used. Simulation run time for dynamic tests were 0,01 seconds and the loads (below in Table 3) were applied in a smooth s-curve during the time of 0,005 seconds.

Table 3 Modeling method comparison test details.

Modeling method	Solids (old)	1D-beams	New method
Tests	Pull, Bend (Figure 18)		
Solvers	OptiStruct (static) & RADIOSS (dynamic)		
Specimen diameter *d* (mm)	10		
Specimen length *L* (mm)	100		
Applied force *F* (kN)	10 (Pull) | 0,25 (Bend)		
Element size (mm)	5 & 10		

Simulation results from the static and dynamic simulations for the new model (displacement) are shown below in Table 4. As you can see, the %-error is quite small, therefore the results are enough accurate for now, as the physical test data is not used yet. Now the model is in good shape to continue refining it with the real data. The reason that there is no result from both 5 mm and 10 mm element size cases, is because with both cases the results were almost identical and therefore, they could be thought as equal. Theoretical result for pull test was calculated with Equation 14 and bend test with Equation 15 [2, p. 47 & 545].

$$\Delta L = \frac{FL}{EA} \tag{14}$$

$$\delta = \frac{FL^3}{3EI} \tag{15}$$

ΔL is longitudinal change in pull test
δ is bending displacement in bend test
F is force applied to the beam
L is length of the test piece
E is Young's modulus of the test piece
A is cross-sectional area of the test piece
I is circle's second moment of area with the respect of central axis

Table 4 Simulation results of the new model compared to theoretical solution.

Case	Theory (mm)	%-error	
		Static (OptiStruct)	Dynamic (RADIOSS)
Bend	2,415	0,295	1,413
Pull	0,1811	0,174	0,119

Time comparison was done between different modeling methods, and you can see from Figure 19 that with dynamic cases, the simulation time differs quite a lot with the usage of different elements, and the new modeling method seemed to perform well against the old method in simulation time, making it more efficient timewise. To be more precise, the new method was 51 % faster on average than the old method. The reason that there is no simulation time comparison shown from static tests, is that the simulation times were identical with all modeling methods (~3 seconds).

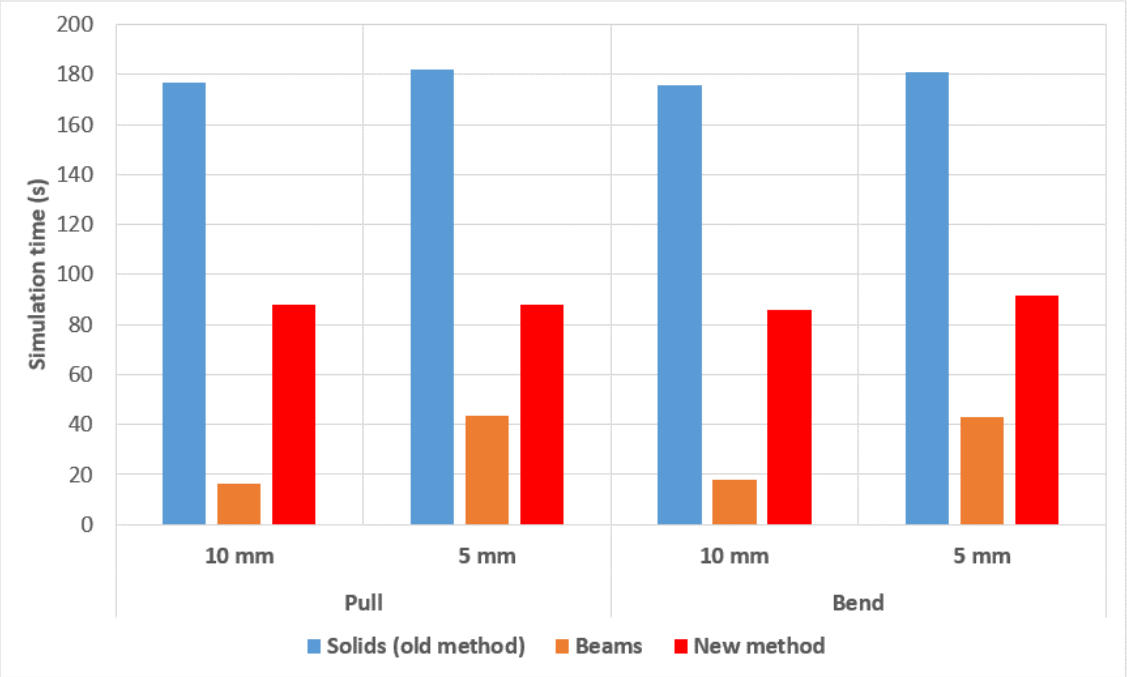

Figure 19 Simulation times (dynamic case) with different modeling methods shown in Figure 17.

6 New cable model testing in simulation environment

The test jigs used in physical testing had to be modeled in simulation environment, but luckily 3D-models of them already existed (as they were designed for these tests). Bending behavior of the cable being much more interesting in the real cases where the model would be used, and with the tensile testing not gone so well, it was decided that the verification of the results would be limited to three-point bend testing, and then move forward to crush testing.

6.1 Setting up the tests in simulation environment

Every jig part that was meshed for the testing, was done as rigid, meaning that the positions of nodes and elements contained in the rigid body remain constant for the whole simulation. Therefore, the elements cannot deform at all. [15] Simulations were performed with forced displacement of the press part. This way the reaction force on the rigids main node was easy to use as an output.

In the three-point bending setup (Figure 20), only small parts of the press part and the support sleds were needed to model.

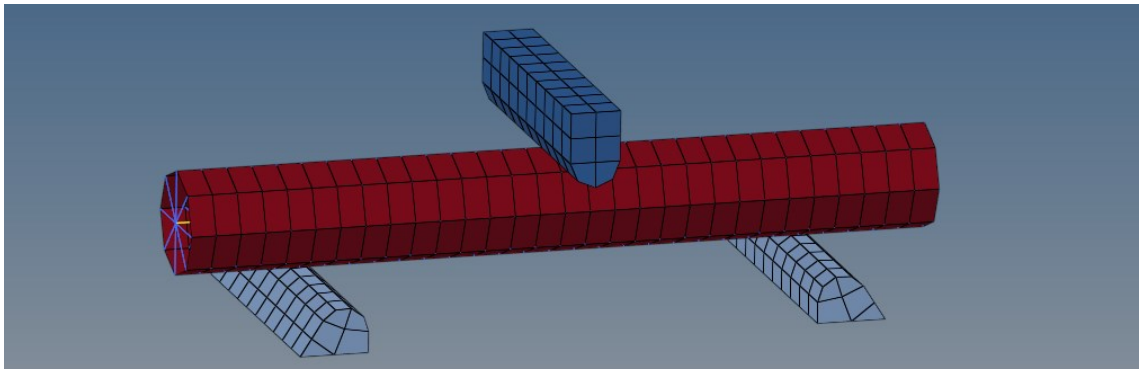

Figure 20 Simulation test setup for three-point bend test.

The same model of the press part was used in crush test setup (Figure 21). For the test, a rigid floor was modeled which the cable could then be crushed against.

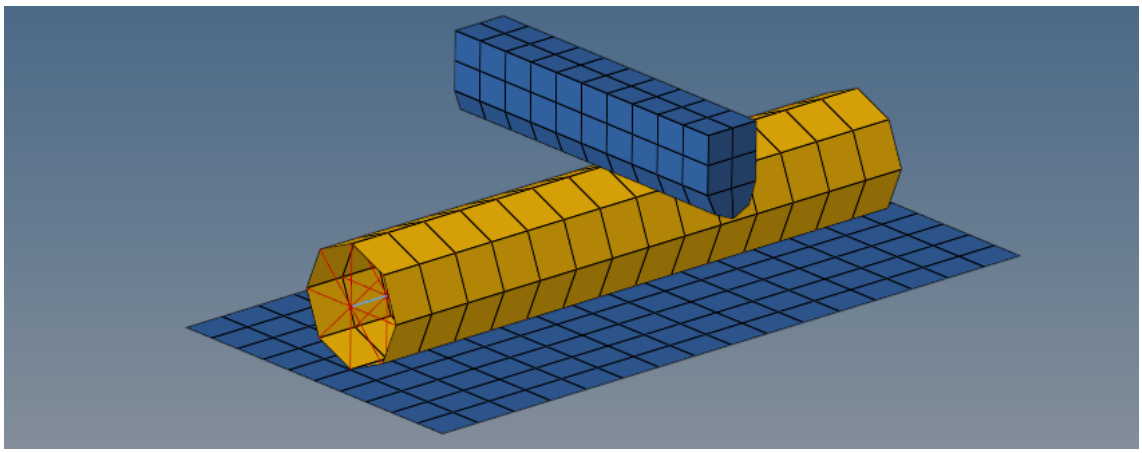

Figure 21 Simulation test setup for crush test.

6.2 Comparing results from physical tests to simulations

As Figure 22 below shows, there was quite much of deviation from the FEA data compared to the physical test data. Overall, the average deviation was 32,73 *N*, but as you can see that the results get closer and closer to the end.

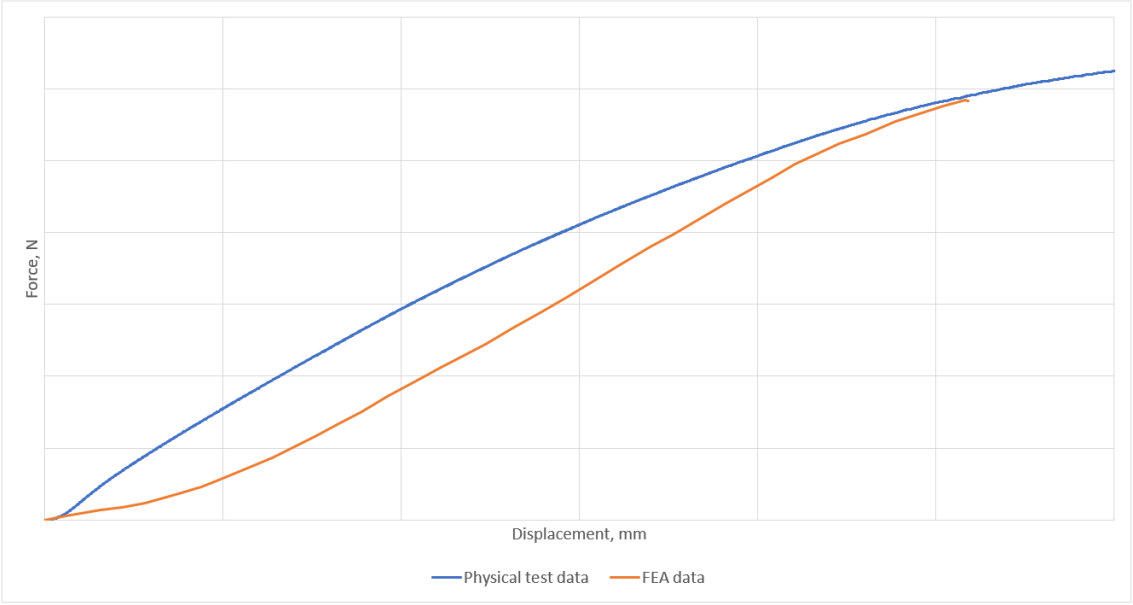

Figure 22 Comparison of physical test data and FEA data of three-point bend testing.

Below in Figure 23, you can see how the new model is deformed during the three-point bend test. Displacement values for the nodes are shown in the form of heat map.

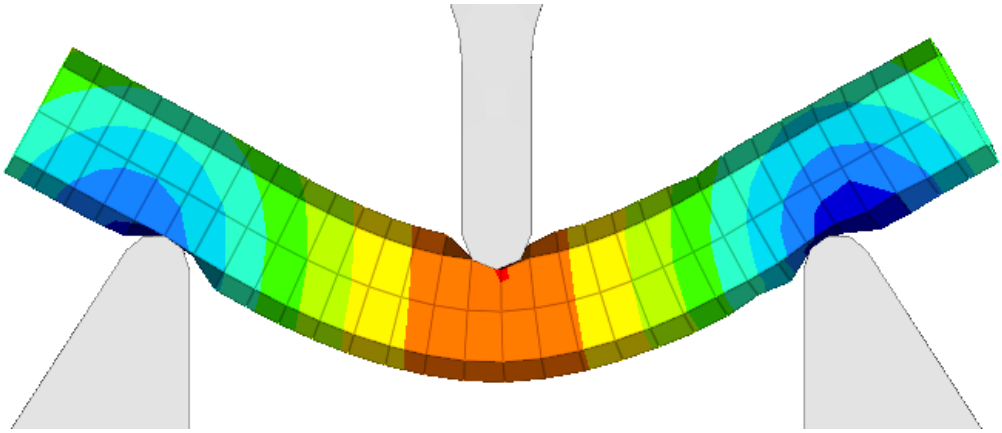

Figure 23 Fully deformed new model in three-point bend test.

The results from crush test can be seen from Figure 24. It can clearly be seen that the FEA data follows the physical test data curves' shape nicely but is deviating just too much to produce acceptable results for now.

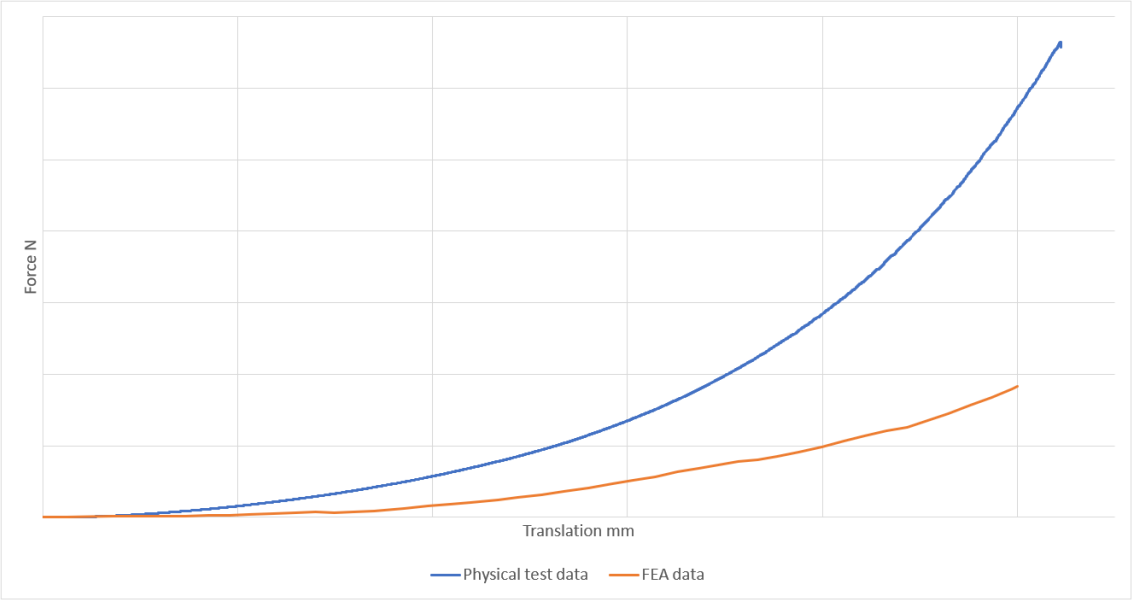

Figure 24 Comparison of physical test data and FEA data of crush testing.

Figure 25 displays the deformation of the new model in crush test. The results in that picture are also the displacement values for the nodes shown in the form of heat map.

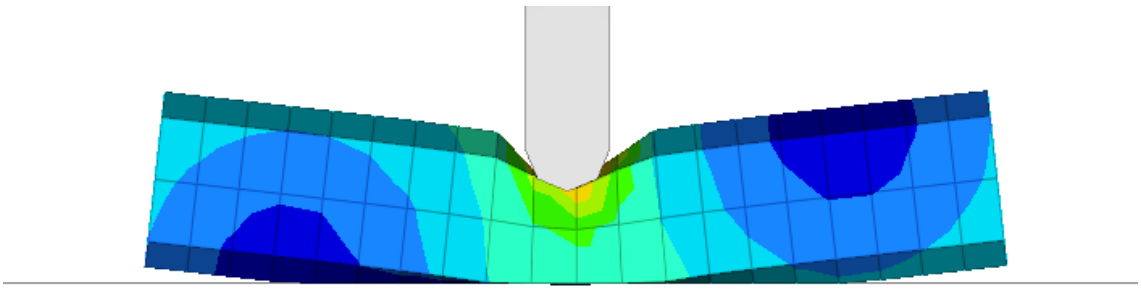

Figure 25 Fully deformed new model in crush test.

7 Results

After performing the tensile tests, some worries about the grip edge on the jaws was recognized - is it too sharp and does it cut the cable during the test. It turned out that this was not the problem, it was the slipping of the top insulating layer. This was solved by stripping that layer off and gripping the cable from the shielding layer. This gave a good grip and somewhat proper results.

Both three-point bend and crush testing went well, and no problems came up. Considering all the tests in general, the deviation of the results was so small, that it could be seen that the test systems were working as intended.

New modeling method for the cables came out as easy and fast to use. One can easily model many cables with the script in the same time, as when one would model one cable with the old method. With the old method one would have to make all kinds of temporary geometry, but with the script one can only select a line and a node and type few values to build the model. It also seemed to perform quite well in the simple simulations performed within this thesis. Modeling in RADIOSS, the mass in elements became a problem. As there is an automatic mass scaling in RADIOSS, it was difficult to determine proper values for the masses without affecting the results too much. This was solved by changing the mass distribution over the elements.

Simulation results of the three-point bend test were surprisingly close to the actual physical test data. But nevertheless, the results from the crush test are too much off to call it a success for now. Now the model needs some refinement, more testing with different parameters and a closer look on how to fit the physical test data together to acquire the best results.

8 Conclusions

What comes to physical testing of the cables, some consideration must be made about the gripping method. Maybe pneumatic or hydraulic gripping or even sturdy enough screw grips might do the job. If the similar tests will be performed in the future, one approach would be to either find a place with these types of gripping methods, or to evaluate if it's worth acquiring some of these options to the internal laboratory for other uses as well.

The thesis brought to light, that investing time to write scripts and use them to speed up pre-processing in FEA, is important and a huge factor of making the most out of the software used. Writing scripts is quite easy, as almost in every FEA-software the program records your every action made. It's easy to write a script with those recorded lines and of course with a little help of basic knowledge in coding (variables and loops etc.).

When comparing the FEA data to the physical test data, there is at least something going as planned, because the FEA curve is following the physical test curve quite nicely. But that doesn't remove the fact that there is a lot of deviation. Some of the input material data is incorrectly converted from the physical test results, leading to too "loose" behavior of the model (not enough stiffness).

There is still some polishing to be done with the methodology to get it to the desired level. This is still a good base to continue developing it. It remains to be seen how the new modeling method performs in a real case, of course, only after when the model is in the desired condition.

References

1 Hosford WF. Mechanical Behavior of Materials. New York: Cambridge University Press; 2009.

2 Karhunen J, Lassila V, Pyy S, Ranta A, Räsänen S, Saikkonen M, Suosara E. Lujuusoppi 543. Helsinki; Espoo: Otatieto Oy; 2019.

3 MechaniCalc, Inc. Basic stress-strain curve for some ductile material with labels. [image on Internet] [cited 2021 Dec 12]. Available from: https://mechanicalc.com/reference/mechanical-properties-of-materials#stress-strain-approx

4 Petrík A, Ároch R. Usage of true stress-strain curve for FE simulation and the influencing parameters. IOP Conference Series: Materials Science and Engineering [Internet] 2019 [cited 2021 Dec 8]; 566:012025. Available from: https://iopscience.iop.org/article/10.1088/1757-899X/566/1/012025/meta#fnref-MSE_566_1_012025bib1 DOI: 10.1088/1757-899X/566/1/012025.

5 Lobo H, Croop B. Determination and Use of Material Properties for Finite Element Analysis. Glasgow: NAFEMS; 2016.

6 Dyson B.F., Gee M.G., Loveday M.S.. Materials Metrology and Standards for Structural Performance. London: Chapman & Hall; 1995.

7 Wai C, Rivai A, Bapokutty O. Modelling optimization involving different types of elements in finite element analysis. IOP Conference Series: Materials Science and Engineering [Internet] 2013 [cited 2022 Feb 11]; 50:012036. Available from: https://iopscience.iop.org/article/10.1088/1757-899X/50/1/012036 DOI: 10.1088/1757-899X/50/1/012036.

8 MatWeb [Internet]. Aluminum 2011-T3. [cited 2022 Feb 11]. Available from: http://www.matweb.com/search/DataSheet.aspx?MatGUID=8c05024423d64aaab0148295c5a57067

9 ASTM International. D790-10. Standard Test Methods for Flexural Properties of Unreinforced and Reinforced Plastics and Electrical Insulating Materials. West Conshohocken: ASTM; 2016.

10 ASTM International. D6272-17e1. Standard Test Method for Flexural Properties of Unreinforced and Reinforced Plastics and Electrical Insulating Materials by Four-Point Bending. West Conshohocken: ASTM; 2020.

11 ASTM International. D695-15. Standard Test Method for Compressive Properties of Rigid Plastics. West Conshohocken: ASTM; 2016.

12 Grasp Engineering [Internet]. Material Properties Required in FEA. [cited 2022 Feb 15]. Available from: https://www.graspengineering.com/material-properties-required-in-fea/

13 Baeker M. How to get meaningful and correct results from your finite element model. [Internet]. 2018 Nov [cited 2022 Feb 15]. Available from: https://www.researchgate.net/publication/328956103_How_to_get_meaningful_and_correct_results_from_your_finite_element_model

14 Altair OptiStruct 2021.2 User Manual. Altair Engineering Inc, 2021.

15 Altair Radioss 2021.2 User Manual. Altair Engineering Inc, 2021.

16 Finnish Standards Association SFS. SFS-EN ISO 6892-1:2019:en. Metallic materials. Tensile testing. Part 1: Method of test at room temperature. Helsinki: SFS; 2019.

17 20kN ProLine operating manual. ZwickRoell GmbH & Co. KG, 2021.

18 Logan D.L. A First Course in the Finite Element Method. 4th ed. London: Thomson Learning; 2007.

19 COMSOL Inc. The first few iterations of a mesh refinement study of a wrench, starting with a very coarse mesh. [image on Internet] [cited 2022 Apr 7]. Available from: https://www.comsol.com/multiphysics/mesh-refinement